

1 **Riparian and in-stream controls on nutrient concentrations and fluxes in a**
2 **headwater forested stream.**

3 **Authors:** S. Bernal^{1,2*}, A. Lupon², M. Ribot¹, F. Sabater², E. Martí¹

4 **Affiliations:**

5 ¹Center for Advanced Studies of Blanes (CEAB-CSIC), Accés a la Cala Sant Francesc
6 14, 17300, Blanes, Girona, Spain.

7 ²Departament d'Ecologia, Facultat de Biologia, Universitat de Barcelona, Av. Diagonal
8 643, 08028, Barcelona, Spain.

9

10 *corresponding author: sbernal@ceab.csic.es

11 **Keywords:** headwater stream, dissolved inorganic nitrogen, phosphorus, longitudinal
12 variation, riparian groundwater, in-stream net nutrient cycling.

13

14 **Abstract**

15 Headwater streams are recipients of water sources draining through terrestrial
16 ecosystems. At the same time, stream biota can transform and retain nutrients dissolved
17 in stream water. Yet, studies considering simultaneously these two sources of variation
18 of stream nutrient chemistry are rare. To fill this gap of knowledge, we analyzed stream
19 water and riparian groundwater concentrations and fluxes as well as in-stream net
20 uptake rates for nitrate (NO_3^-), ammonium (NH_4^+), and soluble reactive phosphorus
21 (SRP) along a 3.7-km reach on an annual basis. Chloride concentrations (used as
22 conservative tracer) indicated a strong hydrological connection at the riparian-stream
23 interface. However, stream and riparian groundwater nutrient concentrations showed a
24 moderate to null correlation, suggesting high in-stream biogeochemical processing. In-
25 stream net nutrient uptake (F_{sw}) was highly variable across contiguous segments and
26 over time, but its temporal variation was not related to the vegetative period of the
27 riparian forest. For NH_4^+ , the occurrence of $F_{sw} > 0 \mu\text{g N m}^{-1} \text{s}^{-1}$ (gross uptake > release)
28 was high along the reach; while for NO_3^- , the occurrence of $F_{sw} < 0 \mu\text{g N m}^{-1} \text{s}^{-1}$ (gross
29 uptake < release) increased along the reach. Within segments and dates, F_{sw} , whether
30 negative or positive, accounted for a median of 6, 18, and 20% of the inputs of NO_3^- ,
31 NH_4^+ , and SRP, respectively. Whole-reach mass balance calculations indicated that in-
32 stream net uptake reduced stream NH_4^+ flux up to 90%, while the stream acted mostly
33 as a source of NO_3^- and SRP. During the dormant period, concentrations decreased
34 along the reach for NO_3^- , but increased for NH_4^+ and SRP. During the vegetative period,
35 NH_4^+ decreased, SRP increased, and NO_3^- showed a U-shaped pattern along the reach.
36 These longitudinal trends resulted from the combination of hydrological mixing with
37 terrestrial inputs and in-stream nutrient processing. Therefore, the assessment of these
38 two sources of variation of stream water chemistry is crucial to understand the

39 contribution of in-stream processes to stream nutrient dynamics at relevant ecological
40 scales.

41 **1. Introduction**

42 Stream water chemistry integrates hydrological and biogeochemical processes
43 occurring within its drainage area and thus, the temporal variation of stream solute
44 concentrations at the catchment outlet is considered a good indicator of the response of
45 terrestrial and aquatic ecosystems to environmental drivers (Bormann and Likens, 1967;
46 Bernhardt et al., 2003; Houlton et al., 2003). Less attention has been paid to the spatial
47 variation of water chemistry along the stream, though it can be considerably important
48 because stream nutrient concentrations are influenced by changes in hydrological flow
49 paths, vegetation cover, and soil characteristics (Dent and Grimm, 1999; Likens and
50 Buso, 2006). For instance, spatial variation in nutrient concentration along the stream
51 has been attributed to changes in soil nitrification rates (Bohlen et al., 2001), soil
52 organic carbon availability (Johnson et al., 2000), and organic soil depth across
53 altitudinal gradients (Lawrence et al., 2000). Moreover, nutrient cycling within the
54 riparian zone can strongly influence stream nutrient concentrations along the stream
55 because these ecosystems are hot spots of biogeochemical processing (McClain et al.,
56 2003; Vidon et al., 2010). In addition, processes occurring at the riparian-stream
57 interface have a larger influence on stream water chemistry than those occurring at
58 catchment locations further from the stream (Ross et al., 2012). Finally, stream
59 ecosystems have a strong capacity to transform and retain nutrients; and thus, in-stream
60 biogeochemical processes can further influence nutrient chemistry along the stream
61 (Peterson et al., 2001; Dent et al., 2007). Therefore, consideration of these multiple
62 sources of variation of stream water chemistry is important to understand drivers of
63 stream nutrient dynamics.

64 Our understanding of nutrient biogeochemistry within riparian zones and
65 streams is mainly based on field studies performed at the plot-scale or in small stream
66 reaches (few hundred meters) (Lowrance et al., 1997; Peterson et al., 2001; Sabater et
67 al., 2003; Mayer et al., 2007; von Schiller et al., 2015). These empirical studies have
68 widely demonstrated the potential of riparian and stream ecosystems as either sinks or
69 sources of nutrients, which ultimately influence the transport of nutrients to downstream
70 ecosystems. Riparian and stream biota are capable of decreasing the concentration of
71 essential nutrients, such as dissolved inorganic nitrogen (DIN) and phosphate,
72 especially with increasing water storage and residence time (Valett et al., 1996; Hedin et
73 al., 1998; Peterson et al., 2001; Vidon and Hill, 2004). Conversely, riparian forests can
74 become sources rather than sinks of nutrients when N₂-fixing species predominate
75 (Helfield and Naiman, 2002; Compton et al., 2003), and in-stream nutrient release can
76 be important during some periods (Bernhardt et al., 2002; von Schiller et al., 2015).
77 Moreover, there is an intimate hydrological linkage between riparian and stream
78 ecosystems that can result in strong biogeochemical feedbacks between these two
79 compartments (e.g., Morrice et al., 1997; Martí et al., 2000; Bernal and Sabater, 2012).
80 However, studies integrating biogeochemical processes of these two nearby ecosystems
81 are rare (but see Dent et al., 2007), and the exchange of water and nutrients between
82 stream and groundwater is unknown in most studies assessing in-stream gross and net
83 nutrient uptake (Roberts and Mulholland, 2007; Covino et al., 2010; von Schiller et al.,
84 2011).

85 There is a wide body of knowledge showing the potential of riparian and stream
86 ecosystems to modify either groundwater or stream nutrient concentrations. Yet, a
87 comprehensive view of the influence of riparian and in-stream processes on stream
88 water chemistry at the catchment scale is still lacking (but see Meyer and Likens, 1979).

89 This gap of knowledge mostly exists because hydrological and biogeochemical
90 processes can vary substantially along the stream (Covino and McGlynn, 2007; Jencso
91 et al., 2010), which limits our ability to extrapolate small plot- and reach- scale
92 measurements to larger spatial scales. Some authors have proposed that nutrient
93 concentrations should decline along the stream if in-stream net uptake is high enough
94 and riparian groundwater inputs are relatively small (Brookshire et al., 2009). This
95 declining pattern is not systematically observed in reach-scale studies, which could
96 bring us to the conclusion that terrestrial inputs are the major driver of stream water
97 chemistry because in-stream gross uptake and release counterbalance each other most of
98 the time (Brookshire et al., 2009). However, synoptic studies have revealed that nutrient
99 concentrations are patchy and highly variable along the stream as a result of spatial
100 patterns in upwelling and in-stream nutrient processing (Dent and Grimm, 1999). Thus,
101 in-stream nutrient cycling could be substantial, but not necessarily lead to longitudinal
102 increases or declines in nutrient concentration, a question that probably needs to be
103 addressed at spatial scales larger than few hundred meters.

104 The goal of this study was to gain a better understanding of the influence of
105 riparian groundwater inputs and in-stream biogeochemical processing on stream
106 nutrient chemistry and fluxes in a headwater forested catchment. To approach this
107 question, we explored the longitudinal pattern of stream nutrient (nitrate, ammonium,
108 and phosphate) concentration along a 3.7-km reach during 1.5 years. We chose a
109 headwater catchment as a model system to investigate drivers of spatial patterns in
110 stream water chemistry because they typically show pronounced changes in riparian and
111 stream features across relatively short distances (Uehlinger, 2000). First, we evaluated
112 riparian groundwater inputs and in-stream nutrient processing as sources of variation of
113 stream nutrient concentration along the reach. We expected stream and riparian

114 groundwater nutrient concentrations to be similar and strongly correlated if riparian
115 groundwater is a major source of nutrients to the stream. In addition, we estimated the
116 in-stream nutrient processing capacity for 14 contiguous segments along the reach with
117 a mass balance approach. Second, we evaluated the relative contribution of riparian
118 groundwater inputs and in-stream biogeochemical processing to stream nutrient fluxes
119 at the whole-reach scale by applying a mass balance approach that include all
120 hydrological input and output fluxes along the reach.

121 **2. Study Site**

122 The research was conducted in the Font del Regàs catchment (14.2 km²) (Figure
123 1), located in the Montseny Natural Park, NE Spain (41°50'N, 2°30'E, 300-1200 m
124 a.s.l.) during the period 2010-2011. Total inorganic N deposition in this area oscillates
125 between 15-30 kg N ha⁻¹ year⁻¹ (Àvila and Rodà 2012). The climate at the Montseny
126 Mountains is subhumid Mediterranean. The long-term mean annual precipitation is
127 925±151 mm and the long-term mean annual air temperature is 12.1±2.5 °C (mean ±
128 SD, period: 1940-2000, Catalan Metereologic Service:
129 <http://www.meteo.cat/servmet/index.html>). During the study period, mean annual
130 precipitation (975 mm) and temperature (12.9 °C) fell within the long-term average
131 (data from a meteorological station within the study catchment). In this period, summer
132 2010 was the driest season (140 mm) while most of the precipitation occurred in winter
133 2010 (370 mm) and autumn 2011 (555 mm) (Figure 2a).

134 The catchment is dominated by biotitic granite (ICC, 2010) and it has steep
135 slopes (28%). Evergreen oak (*Quercus ilex*) and beech (*Fagus sylvatica*) forests cover
136 54% and 38% of the catchment area, respectively (Figure 1). The upper part of the
137 catchment (2%) is covered by heathlands and grasslands (ICC, 2010). The catchment
138 has a low population density (< 1 person km⁻²) which is concentrated in the valley

139 bottom. Hillslope soils (pH ~ 6) are sandy, with high content of rocks (33-36%). Soils at
140 the hillslopes have a 3-cm depth O-horizon and a 5- to 15-cm depth A-horizon
141 (averaged from 10 soil profiles).

142 The riparian zone is relatively flat (slope < 10%), and it covers 6% of the
143 catchment area. Riparian soils (pH ~ 7) are sandy-loam with low rock content (13%)
144 and a 5-cm depth organic layer followed by a 30-cm depth A-horizon (averaged from 5
145 soil profiles). Along the 3.7-km reach, the width of the riparian zone increases from 6 to
146 32 m, whereas the total basal area of riparian trees increases by 12 fold (based on forest
147 inventories of 30-m plots every ca. 150 m) (Figure S1). *Alnus glutinosa*, *Robinia*
148 *pseudoacacia*, *Platanus hybrida*, and *Fraxinus excelsior* are the most abundant riparian
149 tree species followed by *Corylus avellana*, *Populus tremula*, *Populus nigra*, and
150 *Sambucus nigra*. The abundance of N₂-fixing species (*A. glutinosa* and *R.*
151 *pseudoacacia*) increases from 0% to > 60% along the longitudinal profile, (Figure S1).
152 During base flow conditions, riparian groundwater (< 1.5 m from the stream channel)
153 flows well below the soil surface (0.5 ± 0.1 m) and thus, the interaction with the riparian
154 organic soil is minimal (averaged from 15 piezometers, n = 165) (Figure S1). During
155 the period of study, riparian groundwater temperature ranged from 5 to 19.5 °C.

156 The 3.7-km study reach is a 2nd order stream along the first 1.5 km and a 3rd
157 order stream for the remaining 63% of its length. The geomorphology of the stream bed
158 changes substantially with stream order. The stream bed along the 2nd order section is
159 mainly composed of rocks and cobbles (70%) with a small contribution of sand (~
160 10%). At the valley bottom, sands and gravels represent 44% of the stream substrate
161 and the presence of rocks is minor (14%). Mean wetted width and water velocity
162 increase between the 2nd and 3rd order section (from 1.6 to 2.7 m and from 0.24 to 0.35
163 m s⁻¹, respectively) (Figure S1). During the study period, stream water temperature

164 ranged from 5 to 18°C. Stream discharge was low in summer (0.33 mm) and peaked in
165 spring (0.79 mm).

166 **3. Materials and Methods**

167 *3.1. Field sampling and laboratory analysis*

168 We selected 15 sampling sites along the 3.7-km study reach. The distance
169 between consecutive sampling sites ranged from 110 to 600 m (Figure 1). At each
170 sampling site, we installed a 1-m long PVC piezometer (3-cm Ø) in the riparian zone at
171 ~ 1.5 m from the stream channel.

172 For each sampling site, we sampled stream water (from the thalweg) and riparian
173 groundwater every 2 months from August 2010 to December 2011. We used pre-acid
174 washed polyethylene bottles to collect water samples after triple-rinsing them with
175 either stream or groundwater. On each sampling date, we also measured dissolved
176 oxygen concentration (DO, in mg l⁻¹) and water temperature (T, in °C) with a YSI
177 ProODO device in both stream water and in riparian groundwater. We avoided
178 sampling soon after storms to ensure that our measurements were representative of low
179 flow conditions, when the influence of in-stream biogeochemical processes on stream
180 nutrient concentrations and fluxes is expected to be the highest. All field campaigns
181 were performed at least 9 days after storm events, except in October 2011 (Figure 2b,
182 black squares). On each sampling date and at each sampling site, we measured
183 groundwater table elevation (in m below soil surface) with a water level sensor
184 (Eijkelkamp 11.03.30) as well as wetted width (in m), stream discharge (Q , in l s⁻¹), and
185 water velocity (m s⁻¹). Q and water velocity were estimated with the slug-addition
186 technique by adding 1 l of NaCl-enriched solution to the stream (electrical conductivity
187 = 75-90 mS cm⁻¹, n = 11) (Gordon et al., 2004). The uncertainty associated with Q
188 measurements was calculated as the relative difference in Q between pairs of tracer

189 additions under equal water depth conditions (difference < 1 mm). The pairs of data
190 were selected from a set of 126 slug additions and water level measurements obtained
191 from the permanent field stations at Font del Regàs (Lupon, unpublished). The
192 measured uncertainty was relatively small (1.9%, n = 11). On each sampling date, we
193 also collected stream water and measured Q at the four permanent tributaries
194 discharging to Font del Regàs stream, which drained 1.9, 3.2, 1.8, and 1.1 km²,
195 respectively (Figure 1). These data were used for mass balance calculations (see below).
196 Additional stream water samples were collected from a small permanent tributary that
197 drained through an area (< 0.4 km²) with few residences and crop fields for personal
198 consumption.

199 Water samples were filtered through pre-ashed GF/F filters (Whatman®) and
200 kept cold (< 4°C) until laboratory analysis (< 24h after collection). Chloride (Cl⁻) was
201 used as a conservative hydrological tracer and analyzed by ionic chromatography
202 (Compact IC-761, Methrom). Nitrate (NO₃⁻) was analyzed by the cadmium reduction
203 method (Keeney and Nelson 1982) using a Technicon Autoanalyzer (Technicon, 1976).
204 Ammonium (NH₄⁺) was manually analyzed by the salicilate-nitropruside method
205 (Baethgen and Alley 1989) using a spectrophotometer (PharmaSpec UV-1700
206 SHIMADZU). Soluble reactive phosphorus (SRP) was manually analyzed by the acidic
207 molybdate method (Murphy and Riley, 1962) using a spectrophotometer (PharmaSpec
208 UV-1700 SHIMADZU).

209 *3.2. Data analysis*

210 The seasonality of biological activity can strongly affect both riparian
211 groundwater chemistry and in-stream biogeochemical processes (Groffman et al., 1992;
212 Hill et al., 2001). Therefore, the data set was separated in two groups based on sampling
213 dates during the vegetative and dormant period (7 and 4 sampling dates, respectively).

214 As a reference, we considered the vegetative period starting at the beginning of riparian
215 leaf-out (April) and ending at the peak of leaf-litter fall (October), coinciding with the
216 onset and offset of riparian tree evapotranspiration, respectively (Nadal-Sala et al.,
217 2013). During the study period, rainfall was similar between the vegetative and dormant
218 period (775 and 876 mm, respectively).

219

220 *3.2.1. Patterns of stream discharge, riparian groundwater inputs, and stream solute* 221 *concentrations*

222 For each period, we examined the longitudinal pattern of stream discharge,
223 riparian groundwater inputs, and stream solute concentrations along the reach. On each
224 sampling date, we calculated area-specific stream discharge by dividing instantaneous
225 discharge by catchment area (Q' , in mm d^{-1}) at each sampling site. We used Q' rather
226 than Q to be able to compare water fluxes from the 15 nested catchments along the
227 reach. We examined the longitudinal patterns of Q' and stream solute concentration
228 (C_{sw}) by applying regression models (linear, exponential, potential, and logarithmic).
229 Model selection was performed by ordinary least square (Zar, 2010). We referred only
230 to the best fit model in each case.

231 The contribution of net riparian groundwater inputs to surface water along each
232 stream segment (Q_{gw}) was estimated as the difference in Q between consecutive
233 sampling sites (Covino et al., 2010). The empirical uncertainty associated with Q was
234 used to calculate a lower and upper limit of Q_{gw} . We considered that Q_{gw} was
235 representative of the net riparian groundwater flux draining to the stream within each
236 stream segment. We acknowledge that this approach oversimplifies the complex
237 hydrological interactions at the riparian-stream interface because it does not consider
238 concurrent hydrological gains and losses within each segment (Payn et al., 2009), but

239 we consider that it provides a representative estimate at the scale of this study. To
240 investigate the longitudinal pattern of riparian groundwater inputs, we calculated the
241 cumulative area-specific net riparian groundwater input ($\Sigma Q'_{gw}$, in mm d^{-1}) by summing
242 up Q_{gw} from the upstream-most site to each of the downstream segments and dividing it
243 by the cumulative catchment area.

244 For each sampling date, we examined whether the 3.7-km reach was either net
245 gaining or net losing water by comparing concurrent gross hydrological gains and losses
246 over the entire reach (Payn et al., 2009). For this spatial scale, we considered that stream
247 segments exhibiting $Q_{gw} > 0$ contributed to gross hydrological gains ($\Sigma Q_{gw} > 0$) while
248 segments with $Q_{gw} < 0$ contributed to gross hydrological losses ($\Sigma Q_{gw} < 0$). Note that
249 gross riparian groundwater fluxes divided by the total catchment area are equal to $\Sigma Q'_{gw}$
250 at the downstream-most site. For each sampling date, we calculated the relative
251 contribution of different water sources to stream discharge at the downstream-most site
252 (Q_{bot}), with Q_{top}/Q_{bot} , $\Sigma Q_{eff}/Q_{bot}$, and $\Sigma Q_{gw}/Q_{bot}$ for upstream, tributaries and riparian
253 groundwater, respectively.

254

255 3.2.2. Sources of variation of stream nutrient concentration along the reach

256 *Riparian groundwater inputs.*

257 We investigated whether longitudinal patterns in stream solute concentration were
258 driven by riparian groundwater inputs by comparing solute concentrations between
259 stream water and riparian groundwater with a Wilcoxon paired sum rank test. A non-
260 parametric test was used because solute concentrations were not normally distributed
261 (Shapiro-Wilk test, $p < 0.01$ for all study solutes) (Zar, 2010).

262 Moreover, we examined the degree of hydrological interaction at the riparian-
263 stream interface by exploring the relationship between stream and riparian groundwater

264 Cl⁻ concentrations with a Spearman correlation. For each period, we quantified the
 265 difference between Cl⁻ concentrations in the two water bodies by calculating
 266 divergences from the 1:1 line with the relative root mean square error (RRMSE, in %):

$$267 \quad RRMSE = \frac{\sqrt{\sum_{i=1}^n (C_{sw} - C_{gw})^2}}{n \cdot \overline{C_{gw}}} \cdot 100 \quad (1)$$

268 where C_{sw} and C_{gw} are stream and riparian groundwater solute concentrations,
 269 respectively, n is the total number of observations, and $\overline{C_{gw}}$ is the average of C_{gw} . A
 270 strong correlation and a low RRMSE between stream and riparian groundwater Cl⁻
 271 concentrations indicate a strong hydrological connection between the two water bodies.
 272 Similarly, we examined the correlation between stream and riparian groundwater
 273 nutrient concentrations. We expected a weak correlation and a high RRMSE value
 274 between nutrient concentrations measured at the two water bodies if the stream has a
 275 high nutrient processing capacity and in-stream gross uptake and release do not
 276 counterbalance each other.

277 *In-stream nutrient processing.* We investigated the influence of in-stream
 278 biogeochemical processes on the longitudinal pattern of stream nutrient concentrations
 279 by applying a mass balance approach for each individual segment (Roberts and
 280 Mulholland, 2007). For each nutrient, we calculated changes in stream flux between
 281 contiguous sampling sites (F_{sw} , in $\mu\text{g m}^{-1} \text{s}^{-1}$), F_{sw} being the net flux resulting from in-
 282 stream gross uptake and release along a particular stream segment (von Schiller et al.,
 283 2011). We expressed F_{sw} by unit of stream length in order to compare net changes in
 284 stream flux between segments differing in length. For each sampling date and for each
 285 nutrient, F_{sw} was approximated with:

$$286 \quad F_{sw} = (F_{top} + F_{ef} + F_{gw} - F_{bot}) / x, \quad (2)$$

287 where F_{top} and F_{bot} are the nutrient flux at the top and at the bottom of each stream
288 segment, F_{gw} is the nutrient flux from net riparian groundwater inputs, and F_{ef} is the
289 nutrient flux from tributary inputs for those reaches including a tributary (all in $\mu\text{g s}^{-1}$)
290 (Figure 3). F_{top} and F_{bot} were calculated by multiplying Q by C_{sw} at the top and at the
291 bottom of the segment, respectively. F_{gw} was estimated by multiplying net groundwater
292 inputs (Q_{gw}) by nutrient concentration in either riparian groundwater or stream water.
293 For net gaining segments ($Q_{gw} > 0$), we assumed that the chemistry of net water inputs
294 was similar to that measured in riparian groundwater and thus, C_{gw} was the average
295 between riparian groundwater nutrient concentration at the top and bottom of the reach.
296 For net losing segments ($Q_{gw} < 0$), we assumed that the chemistry of net water losses
297 was similar to that measured in stream water and thus, C_{gw} averaged stream water
298 concentration at the top and at the bottom of each reach segment (C_{top} and C_{bot} ,
299 respectively). For those cases in which stream segments received water from a tributary,
300 F_{ef} was calculated by multiplying Q and C at the outlet of the tributary. We calculated
301 an upper and lower limit of F_{sw} based on the empirical uncertainty associated with water
302 fluxes (Q and Q_{gw}). Finally, x (in m) is the length of the segment between two
303 consecutive sampling sites. The same approach was applied for Cl^- , a conservative
304 tracer that was used as a hydrological reference. For Cl^- , we expected $F_{sw} \sim 0$ if inputs
305 from upstream, tributaries, and riparian groundwater account for most of the stream Cl^-
306 flux. For nutrients, F_{sw} can be positive (gross uptake $>$ release), negative (gross uptake $<$
307 release) or nil (gross uptake \sim release). Therefore, we expected $F_{sw} \neq 0$ if in-stream
308 gross uptake and release processes do not fully counterbalance each other (von Schiller
309 et al., 2011). To investigate whether stream segments were consistently acting as net
310 sinks or net sources of nutrients along the stream during the study period, we calculated
311 the frequency of $F_{sw} > 0$, $F_{sw} < 0$, and $F_{sw} = 0$ for each nutrient and for each segment..

312 We assumed that F_{sw} was undistinguishable from 0 when its upper and lower limit
313 contained zero.

314 Since in-stream nutrient cycling can substantially vary with reach length (Meyer
315 and Likens, 1979; Ensign and Doyle, 2006), we also calculated F_{sw} for the whole 3.7-
316 km reach by including all hydrological input and output fluxes (solute fluxes from the
317 upstream-most site, tributaries, and riparian groundwater gross gains and losses) in a
318 mass balance at the whole-reach scale. For the two spatial scales (segment and whole
319 reach), we examined whether F_{sw} differed among nutrients with a Mann Whitney test.

320

321 *3.2.3. Relative contribution of riparian groundwater and in-stream nutrient processing* 322 *to stream nutrient fluxes*

323 To assess the relevance of F_{sw} compared to input solute fluxes, we calculated the
324 ratio between $F_{sw} \cdot x$ (absolute value) and the total input flux (F_{in}) for each solute and
325 sampling date. For the two spatial scales (segment and whole reach), F_{in} was the sum of
326 upstream (F_{top}), tributaries (F_{ef}), and net riparian groundwater inputs (F_{gw}). The latter
327 was included when $Q_{gw} > 0$. We interpreted a high $|F_{sw} \cdot x / F_{in}|$ ratio as a strong potential
328 of in-stream processes to modify input fluxes (either as a consequence of gross uptake
329 or release). For each spatial scale, we explored whether $|F_{sw} \cdot x / F_{in}|$ differed among
330 nutrients with a Mann Whitney test.

331 We used a whole-reach mass balance approach to assess the relative contribution
332 of net riparian groundwater inputs ($(F_{gw} > 0) / F_{in}$) and in-stream release
333 ($|(F_{sw} < 0) / F_{in}|$) to stream solute fluxes. In addition, we calculated the contribution of
334 upstream (F_{top} / F_{in}) and tributary inputs (F_{ef} / F_{in}) to stream solute fluxes. For each solute,
335 we analyzed differences in the relative contribution of different sources to stream input
336 fluxes with a Mann Whitney test. Finally, when the whole reach was acting as a net sink

337 for a particular nutrient ($F_{sw} > 0$), we calculated the relative contribution of in-stream
338 net uptake to reduce stream nutrient fluxes along the 3.7-km reach with $F_{sw \cdot x} / F_{in}$.

339 **4. Results**

340 *4.1. Hydrological characterization of the stream reach*

341 During the study period, mean Q' decreased from 0.82 ± 0.13 [mean \pm SE] to
342 0.54 ± 0.11 mm d⁻¹ along the reach (linear regression [l.reg], $r^2 = 0.79$, degrees of
343 freedom [df] = 14, $F = 51.4$, $p < 0.0001$) (Figure 4a). This pattern hold for the two
344 seasonal periods considered (dormant and vegetative; Wilcoxon rank sum test, $p >$
345 0.05).

346 On average, the stream was net gaining water along the 3.7-km reach, though the
347 hydrological interaction between the riparian zone and the stream was highly variable
348 across contiguous segments (Figure 4b). The stream was consistently gaining water
349 along the first 1.5 km and the last 0.5 km, while hydrological losses were evident along
350 the intermediate 2 km (Figure 4b). At the whole-reach scale, gross hydrological gains
351 exceed gross losses in 8 out of 10 field dates (Figure 2c and d). This was especially
352 noticeable in April and December 2011, the two sampling dates most influenced by
353 storm events. In contrast, the whole reach was acting as net hydrological losing in
354 March and October 2011.

355 Stream Cl⁻ concentrations showed a 40% increase along the reach (l.reg, $r^2 =$
356 0.88 , $df = 14$, $F = 44.6$, $p < 0.0001$), which contrasted with the longitudinal pattern
357 exhibited by stream discharge (Figure 4c). The two periods showed a similar
358 longitudinal pattern, though stream Cl⁻ concentration was lower during the dormant than
359 during the vegetative period (Wilcoxon rank sum test, $Z = -6.4$, $p < 0.0001$) (Table 1).
360 The same seasonal pattern was exhibited by the five permanent tributaries (Figure 4c).

361 There was a strong correlation between stream and riparian groundwater Cl⁻
362 concentrations, which fitted well to the 1:1 line (low RRMSE for the two periods)
363 (Table 2 and Figure S2).

364 The mean net change in Cl⁻ flux within individual segments was $0.4 \pm 0.03 \text{ mg}$
365 $\text{m}^{-1} \text{ s}^{-1}$, which represented a small fraction of the Cl⁻ input flux ($|F_{sw} \cdot x / F_{in}| < 6 \%$).
366 Similar results were obtained when calculating Cl⁻ budgets for the whole-reach
367 approach (Table 3). The stream Cl⁻ flux was mainly explained by inputs from tributaries
368 followed by riparian groundwater and upstream (Table 4). Similar results were obtained
369 when calculating the relative contribution of different water sources to stream discharge
370 at the whole-reach scale.

371 *4.2. Longitudinal pattern of stream nutrient concentration*

372 The longitudinal pattern of stream concentration differed between nutrients and
373 periods. During the dormant period, stream NO₃⁻ concentration decreased along the
374 reach especially within the first 1.5 km (l.reg, $r^2 = 0.47$, $df = 15$, $F = 11.4$, $p < 0.005$)
375 (Figure 5a). During the vegetative period, stream NO₃⁻ concentration showed a U-
376 shaped pattern: it decreased along the first 1.5 km, remained constant along the
377 following 1 km, and increased by 60% along the last km of the reach (Figure 5a).
378 Despite these differences, stream NO₃⁻ concentration was similar between the dormant
379 and vegetative period for both the main stream and tributaries (in all cases, Wilcoxon
380 rank sum test, $p > 0.05$) (Table 1).

381 Stream NH₄⁺ concentration showed an increasing longitudinal pattern during the
382 dormant period (exponential regression [e.reg], $r^2 = 0.45$, $df = 15$, $F = 10.5$, $p < 0.01$),
383 while concentration decreased during the vegetative period (logarithmic regression
384 [lg.reg], $r^2 = 0.42$, $df = 15$, $F = 9.6$, $p < 0.01$) (Figure 5b). The main stream showed

385 higher NH_4^+ concentration during the vegetative than during the dormant period
386 (Wilcoxon rank sum test, $Z_{\text{NH}_4} = -3.5$, $p < 0.001$) (Table 1). For the tributaries, NH_4^+
387 concentration was similar between the two periods (in all cases, Wilcoxon rank sum
388 test, $p > 0.01$).

389 Stream SRP concentration increased along the reach during both the dormant
390 (e.reg, $r^2 = 0.59$, $F = 18.5$, $df = 14$, $p < 0.01$) and vegetative period (l.reg, $r^2 = 0.49$, $F =$
391 12.4 , $df = 14$, $p < 0.01$) (Figure 5c). Similarly to NH_4^+ , the main stream showed higher
392 SRP concentration during the vegetative than during the dormant period (Wilcoxon rank
393 sum test, $Z_{\text{SRP}} = -6.6$, $p < 0.001$) (Table 1). For the tributaries, SRP concentration was
394 similar between the two periods (in all cases, Wilcoxon rank sum test, $p > 0.01$).

395 *4.3. Sources of variation of stream nutrient concentration*

396 *Riparian groundwater inputs.* The relationship between stream and riparian
397 groundwater concentrations differed between nutrients and periods. During the dormant
398 period, stream and riparian groundwater NO_3^- concentrations were similar, while the
399 stream showed higher concentration during the vegetative period (Table 1). During the
400 two periods, stream and riparian groundwater NO_3^- concentrations were positively
401 correlated and showed relatively small RRMSE (Table 2 and Figure S2). NH_4^+
402 concentration in stream water was 2-3 times lower than in riparian groundwater (Table
403 1), and stream and groundwater concentrations were no correlated either during the
404 dormant or vegetative periods (Table 2). Stream and riparian groundwater SRP
405 concentrations were similar in the two periods (Table 1). During the dormant period,
406 SRP concentration showed a significant correlation between the two water bodies, while
407 no correlation and relatively high RRMSE occurred during the vegetative period (Table
408 2). The differences in nutrient concentrations between stream and riparian groundwater

409 in the two study periods were accompanied by consistently higher DO concentrations in
410 the stream than in riparian groundwater (Table 1).

411 *In-stream nutrient processing.* The influence of in-stream nutrient processing on
412 stream water chemistry differed among nutrients. During the study period, median F_{sw}
413 was negative for NO_3^- , positive for NH_4^+ , and close to 0 for SRP (Table 3). Yet,
414 between-nutrient differences in F_{sw} were not statistically significant for either the
415 vegetative or dormant period (for both periods: Mann Whitney test with post-hoc Tukey
416 test, $p > 0.05$). Similar F_{sw} values were obtained when calculating nutrient budgets
417 either by segment or whole reach (Table 3).

418 The frequency of an individual segment to act either as a nutrient sink or source
419 differed among nutrients and along the reach. For NO_3^- , the frequency of $F_{sw, \text{NO}_3} < 0$
420 (gross uptake < release) increased from 9 to > 50% along the reach (l.reg, $r^2 = 0.55$, $df =$
421 13, $F = 14.67$, $p < 0.01$) (Figure 6a). For NH_4^+ , the frequency of $F_{sw, \text{NH}_4} > 0$ (gross
422 uptake > release) was high across individual segments, ranging from 20 to 90% (Figure
423 6b). For SRP, the frequency of $F_{sw, \text{SRP}} < 0$, > 0 , or ~ 0 did not show any consistent
424 longitudinal pattern (Figure 6c). Overall, the frequency of sampling dates for which in-
425 stream biogeochemical processes were imbalanced ($F_{sw} \neq 0$) was lower for NO_3^- (36%)
426 than for NH_4^+ (80%) and SRP (68%) (Figure 6).

427 *4.4. Relative contribution of riparian groundwater and in-stream processing to stream* 428 *nutrient fluxes at the segment and whole-reach scale*

429 The capacity of in-stream processes to modify stream input fluxes differed
430 between nutrients and spatial scales. For individual segments, $|F_{sw} \cdot x / F_{in}|$ was smaller for
431 NO_3^- (6%) than for NH_4^+ and SRP (~20%) (Mann Whitney test with post-hoc Tukey

432 test, $p < 0.01$, Table 3). However, $|F_{sw} \cdot x / F_{in}|$ increased substantially for NO_3^- and NH_4^+
433 when nutrient budgets were calculated at the whole-reach scale (Table 3).

434 According to whole-reach mass balance calculations, the stream acted as a net
435 source of NO_3^- on 7 out of the 10 sampling dates for which whole-reach budgets were
436 calculated. The contribution of in-stream release to stream NO_3^- fluxes was as important
437 as that of riparian groundwater and upstream fluxes (Table 4). In-stream net NO_3^-
438 retention at the whole-reach scale was observed only in spring (March and April 2011)
439 and December 2011 (Figure 7a).

440 In contrast to NO_3^- , the stream generally acted as a net sink of NH_4^+ and it
441 retained up to 90% of the input fluxes in spring and autumn (Figure 7b). The stream
442 acted as a source of NH_4^+ in summer (Figure 7b), though the contribution of in-stream
443 release to stream NH_4^+ fluxes was minimal compared to that from riparian groundwater
444 (Table 4).

445 The stream acted as a net source of SRP in 6 out of the 10 sampling dates. The
446 contribution of in-stream release to stream SRP fluxes was as important as that of
447 riparian groundwater (Table 4). In-stream net SRP retention was minimal, except in
448 autumn 2011 (October and December 2011) (Figure 7c).

449 **5. Discussion**

450 In terms of hydrology, the study headwater stream was a net gaining reach,
451 though the hydrological interaction between the riparian zone and the stream was
452 complex as indicated by the longitudinal variation in net riparian groundwater inputs.
453 Moreover, the longitudinal decrease in area-specific discharge suggests that
454 hydrological retention increased at the valley bottom compared to upstream segments as
455 reported in previous studies (Covino et al., 2010). Despite the complex hydrological

456 processes along the reach, the strong positive correlation between stream and riparian
457 groundwater Cl^- concentration suggests high hydrological connectivity at the riparian-
458 stream interface (Butturini et al., 2003). In addition, we found that the permanent
459 tributaries, which comprised $\sim 50\%$ of the catchment area, contributed 56% of stream
460 discharge; and thus, they were an essential piece to understand stream nutrient
461 chemistry and loads. Hydrological mixing of stream water with water from tributaries
462 could partially explain the longitudinal increase in Cl^- because its concentration was
463 higher at the tributaries than at the main stream, especially during the vegetative period.
464 In addition, riparian groundwater inputs to the stream could further contribute to the
465 longitudinal increase in stream Cl^- concentration because they contributed 26% of
466 stream discharge and also exhibited higher Cl^- concentration than stream water.

467 Based on the strong hydrological connectivity between the stream and the
468 riparian groundwater and the large contribution of tributaries to stream discharge, one
469 would expect a strong influence of these water sources on the longitudinal variation of
470 stream nutrient chemistry. However, the relationship between stream and riparian
471 groundwater nutrient concentration was from moderate to weak for NO_3^- and SRP, and
472 nil for NH_4^+ . Further, the contribution of tributaries to stream nutrient fluxes was
473 relatively small (from 21 to 34%) compared to their contribution to stream Cl^- and water
474 fluxes ($> 50\%$). Together these data suggest that longitudinal patterns of stream nutrient
475 concentration could not be explained by hydrological mixing alone; and thus, pointed at
476 in-stream biogeochemical processing as a likely mechanism to modify nutrient
477 concentrations along the study reach. In fact, the estimates of in-stream net nutrient
478 uptake (F_{sw}) at the different stream segments supported this idea and agreed with
479 previous studies showing that in-stream processes can mediate stream nutrient

480 chemistry and downstream nutrient export (McClain et al., 2003; Harms and Grimm,
481 2008).

482 Our results revealed an extremely high variability in F_{sw} , that could range up to
483 one order of magnitude, across individual segments and over time, which agrees with
484 findings from other headwater streams (von Schiller et al., 2011). However, some
485 general trends aroused when comparing patterns for the different studied nutrients. For
486 instance, the frequency of dates for which in-stream gross uptake and release were
487 imbalanced ($F_{sw} \neq 0$) was higher for NH_4^+ (80%) and SRP (68%) than for NO_3^- (37%).
488 Further, the potential of in-stream processes to modify stream fluxes within stream
489 segments ($|F_{sw} \cdot x / F_{in}|$) was 3 fold higher for NH_4^+ and SRP than for NO_3^- . Our findings
490 are concordant with studies performed at short stream reaches (< 300 m) worldwide,
491 which show that in-stream gross uptake velocity (as a proxy of nutrient demand) is
492 typically higher for NH_4^+ and SRP than for NO_3^- (Ensign and Doyle, 2006). This
493 difference among nutrients is commonly attributed to the higher biological demand for
494 NH_4^+ and SRP than for NO_3^- . However, we found that F_{sw} was similar among nutrients;
495 and thus, differences in $|F_{sw} \cdot x / F_{in}|$ were mainly associated with differences in the
496 concentration of the inputs, which tend to be 20 fold lower for NH_4^+ and SRP than for
497 NO_3^- . Divergences between F_{sw} and $|F_{sw} \cdot x / F_{in}|$ were even more remarkable when
498 nutrient budgets were considered at the whole-reach scale, especially for DIN forms.
499 NO_3^- and NH_4^+ showed no differences in F_{sw} between the two scales of observation;
500 however, they showed a substantial increase in $|F_{sw} \cdot x / F_{in}|$ at the whole-reach scale
501 (length of kilometers) compared to the segment scale (length of hundreds of meters).
502 Similarly, previous nutrient spiraling studies have reported an increase in the proportion
503 of nutrient removal with stream order despite no changes in gross uptake rates among
504 stream reaches (Ensign and Doyle, 2006; Wollheim et al., 2006). This pattern has been

505 attributed to variation in intrinsic stream characteristics, such as stream nutrient
506 concentration, discharge, stream width, and the size of the hyporheic zone (Wollheim et
507 al., 2006; Alexander et al., 2009), which may also hold for our study since these
508 characteristics varied along the 3.7-km reach. However, our results also indicate that the
509 assessment of riparian groundwater inputs is crucial to understand the contribution of
510 in-stream processes to stream nutrient fluxes. Overall, our findings add to the growing
511 evidence that streams are hot spots of nutrient processing (Peterson et al., 2001; Dent et
512 al., 2007), and that in-stream processes can substantially modify stream nutrient fluxes
513 at the catchment scale (Ensign and Doyle, 2006; Bernal et al., 2012).

514 The potential of in-stream processes to regulate stream nutrient fluxes was
515 especially remarkable for NH_4^+ . There was no relationship between stream and riparian
516 groundwater NH_4^+ concentrations; and further, whole-reach budgets indicated that in-
517 stream net uptake could reduce the flux of NH_4^+ up to 90% along the reach. This high
518 in-stream bioreactive capacity could be favored by the sharp increase in redox
519 conditions from riparian groundwater to stream water (Hill et al., 1998; Dent et al.,
520 2007). Concordantly, NH_4^+ concentrations were higher in riparian groundwater than in
521 the stream, while the opposite occurred for NO_3^- (although only during the vegetative
522 period). These results suggest fast nitrification of groundwater inputs within the stream
523 as environmental conditions become well oxygenated (Jones et al., 1995). Supporting
524 this idea, we found that in-stream gross NH_4^+ uptake prevailed over release along the
525 reach. However, the marked increase in stream NO_3^- concentration observed along the
526 last 700 m of the reach during the vegetative period could not be explained entirely by
527 nitrification of riparian groundwater NH_4^+ because this flux ($F_{gw,NH4} \sim 2 \mu\text{g N m}^{-1} \text{ s}^{-1}$)
528 was not large enough to sustain in-stream NO_3^- release $|F_{sw,NO3} < 0|$ ($\sim 10 \mu\text{g N m}^{-1} \text{ s}^{-1}$).
529 This finding suggests an additional source of N at the valley bottom. Previous studies

530 have shown that leaf litter from riparian trees, and especially from N₂-fixing species,
531 can enhance in-stream nutrient cycling because of its high quality and edibility (Starry
532 et al., 2005; Mineau et al., 2011). Thus, the increase in NO₃⁻ and SRP concentrations
533 and in-stream NO₃⁻ release observed at the lowest part of the catchment during the
534 vegetative period could result from the combination of warmer temperatures and the
535 mineralization of large stocks of alder and black locust leaf litter stored in the stream
536 bed (Strauss and Lamberti, 2000; Bernhardt et al., 2002; Starry et al., 2005).

537 Alternatively, increases in stream NO₃⁻ and SRP concentration could result from human
538 activities, which were concentrated at the lowest part of the catchment. However,
539 regarding NO₃⁻, anthropogenic sources seem unlikely because DIN concentrations at the
540 tributary draining through the inhabited area were low. In contrast, this tributary showed
541 high SRP concentrations (from 2 to 6 fold higher than in the main stream), though its
542 discharge should have had to be ca. 4 times higher than expected for its drainage area (<
543 0.4 km²) to explain the observed changes in concentration. Another possible explanation
544 for the increase in stream N concentration at the valley bottom could be increased N
545 fixation by stream algae (Finlay et al., 2011). However, in-stream DIN release (NO₃⁻
546 and NH₄⁺) peaked in late spring and summer (May and August 2011), when light
547 penetration was limited by riparian canopy and in-stream photoautotrophic activity was
548 low (Lupon et al., 2015). Altogether, these data suggest that the sharp increase in
549 nutrient availability along the last 700 m of the reach was likely related to the massive
550 presence of the invasive black locust at the valley bottom. Black locust is becoming
551 widespread throughout riparian floodplains in the Iberian Peninsula (Castro-Díez et al.,
552 2014) and its potential to subsidize N to stream ecosystems via root exudates and leaf
553 litter could dramatically alter in-stream nutrient processing and downstream nutrient
554 export (e.g., Stock et al., 1995; Mineau et al., 2011). However, further research is

555 needed to test the hypothesis that this invasive species can alter stream nutrient
556 dynamics in riparian floodplains.

557 It is worth noting that longitudinal trends in stream nutrient concentrations
558 showed no simple relationship to in-stream processes. This finding evidenced that other
559 sources of variation of stream water chemistry were counterbalancing the influence of
560 in-stream processes on stream nutrient fluxes. In this sense, results from NH_4^+ were
561 paradigmatic. The mass balance approach clearly showed that in-stream gross uptake of
562 NH_4^+ exceeded release; and concordantly, NH_4^+ concentration was consistently lower in
563 the stream than in riparian groundwater. Yet, stream NH_4^+ concentration showed small
564 longitudinal variation likely because in-stream net uptake balanced the elevated inputs
565 from riparian groundwater. Therefore, our results challenge the idea that stream nutrient
566 concentration should decrease in the downstream direction when in-stream processes
567 are efficient in taking up nutrients from receiving waters (Brookshire et al., 2009).
568 Conversely, our findings convincingly show that in-stream processes can strongly affect
569 stream nutrient chemistry and downstream nutrient export even in the absence of
570 consistent longitudinal gradients in nutrient concentration. For NO_3^- , our data suggest
571 that the marked increase in concentration along the last 700 m could be a consequence
572 of in-stream mineralization of N-rich leaf-litter stocks. However, the observed decrease
573 in NO_3^- concentration along the first 1.5 km of the reach could be barely explained by
574 in-stream processing alone because its contribution to reduce stream NO_3^- fluxes was
575 too low, even when the whole-reach budget was recalculated excluding the last 700 m
576 of the reach ($F_{sw} = 0.61 \mu\text{g N m}^{-1} \text{ s}^{-1}$ and $(F_{sw} > 0)/F_{in} = 10\%$). Therefore, the
577 declining pattern was likely a combination of both in-stream nutrient processing and
578 hydrological mixing with riparian groundwater and tributary inputs. For SRP, the
579 longitudinal increase in concentration could neither be fully explained by in-stream

580 release because $F_{sw,SRP} < 0$ was not widespread along the reach and the stream only
581 contributed to input fluxes by 19% (6% when excluding the last 700 m). Again, stream
582 nutrient chemistry along the reach was the combination of both in-stream nutrient
583 processing and hydrological mixing as indicated by our whole-reach mass balance.
584 Recent studies have concluded that riparian groundwater is a major driver of
585 longitudinal patterns in stream nutrient concentration in headwater streams (Bernhardt
586 et al., 2002; Asano et al., 2009; Scanlon et al., 2010). Our study adds to our knowledge
587 of catchment biogeochemistry by showing that stream nutrient chemistry results from
588 the combination of both hydrological mixing from the riparian zone and in-stream
589 nutrient processing, which can play a pivotal role on shaping stream nutrient
590 concentrations and fluxes at the catchment scale.

591 **6. Conclusions**

592 The synoptic approach adopted in this study highlighted that the Font del Regàs
593 stream had a strong potential to transform nutrients. Longitudinal pattern in stream
594 nutrient concentrations could not be explained solely by hydrological mixing with
595 riparian groundwater and tributary sources because dissolved nutrients underwent
596 biogeochemical transformation while travelling along the stream channel. Our results
597 revealed that in-stream processes were highly variable over time and space, though in
598 most cases this variability could not be associated with either physical longitudinal
599 gradients or shifts in environmental conditions between the dormant and vegetative
600 period. Nevertheless, results from a mass balance approach showed that in-stream
601 processes contributed substantially to modify stream nutrient fluxes and that the stream
602 could act either as a net nutrient sink (for NH_4^+) or as a net nutrient source (for SRP and
603 NO_3^-) at the catchment scale. These results add to the growing evidence that in-stream
604 biogeochemical processes may be taken into consideration in either empirical or

605 modeling approaches if we are to understand drivers of stream nutrient chemistry within
606 catchments.

607 Recent studies have proposed that riparian groundwater is a major control of
608 longitudinal patterns of nutrient concentration because in-stream gross nutrient uptake
609 and release tend to counterbalance each other most of the time (Brookshire et al., 2009;
610 Scanlon et al., 2010). Conversely, our study showed that in-stream processes can
611 influence stream nutrient chemistry and downstream exports without generating
612 longitudinal gradients in concentration and flux because changes in stream nutrient
613 chemistry are the combination of both in-stream processing and nutrient inputs from
614 terrestrial sources. Our results imply that the assessment of these two sources of
615 variation of stream nutrient chemistry is crucial to understand the contribution of in-
616 stream processes to stream nutrient dynamics at relevant ecological scales.

617 Reliable measurements of riparian groundwater inputs are difficult to obtain
618 because spatial variability can be high (Lewis et al., 2006) and to determine the
619 chemical signature of the groundwater that really enters the stream is still a great
620 challenge (Brookshire et al., 2009). In this study, we installed 15 piezometers along the
621 reach (one per sampling site) which may not be representative enough of the variation
622 of riparian groundwater chemistry. However, and despite its limitations, riparian
623 groundwater sampling near the stream can help to constrain the uncertainty associated
624 with this water source and provide more reliable estimations of in-stream net nutrient
625 uptake for both nutrient mass balance and spiraling empirical approaches (von Schiller
626 et al., 2011).

627 **Author contribution**

628 S.B., F.S., and E.M. designed the experiment. S.B, A.L., M.R., and F.S. carried
629 them out. A.L. performed all laboratory analysis. S.B. analyzed the data set and
630 prepared the manuscript with contributions from A.L., M.R., and E.M.

631 **Acknowledgements**

632 We are grateful to three anonymous reviewers for their helpful comments on an
633 earlier version of the manuscript, and in particular to one of them for his constructive
634 and meaningful suggestions. We thank A. Oltra for assisting with GIS, and S. Poblador,
635 E. Martín, and C. Romero for field assistance. S.B. and A.L. were funded by the
636 Spanish Ministry of Economy and Competitiveness (MINECO) with a Juan de la Cierva
637 contract (JCI-2010-06397) and a FPU grant (AP-2009-3711). S.B received additional
638 funds from the Spanish Research Council (CSIC) (JAEDOC027) and the MICECO-
639 funded project MED_FORESTREAM (CGL2011-30590). M. Ribot was funded by a
640 technical training contract from the MINECO-funded project ISONEF (CGL2008-
641 05504-C02-02/BOS) and MED_FORESTREAM. Additional financial support was
642 provided by the European Union-funded project REFRESH (FP7-ENV-2009-1-244121)
643 and the MINECO-funded project MONTES-Consolider (CSD 2008-00040). The Vichy
644 Catalan Company, the Regàs family and the Catalan Water Agency (ACA) graciously
645 gave us permission for at the Font del Regàs catchment.

646 **References**

647 Alexander, R. B., Böhlke, J. K., Boyer, E. W., David, M. B., Harvey, J. W.,
648 Mulholland, P. J., Seitzinger, S. P., Tobias, C. R., Tonitto, C., and Wollheim, W. M..
649 Dynamic modeling of nitrogen losses in river networks unravels the coupled effects
650 of hydrological and biogeochemical processes. *Biogeochemistry*, 93, 91-116, 2009.

651 Asano, Y., Uchida, T.M., Mimasu, Y., and Ohte, N. Spatial patterns of stream solute
652 concentrations in a steep mountainous catchment with a homogeneous landscape.
653 *Water Resour. Res.*, 45, W10432, doi: 10.1029/2008WR007466, 2009.

654 Àvila, A., and Rodà, F. Changes in atmospheric deposition and streamwater chemistry
655 over 25 years in undisturbed catchments in a Mediterranean mountain environment.
656 *Sci. Total Environ.*, 434, 18-27, 2012.

657 Baethgen, W., and Alley, M. A manual colorimetric procedure for ammonium nitrogen
658 in soil and plant Kjeldahl Digests. *Commun. Soil Sci. Plan.*, 20, 961–969, 1989.

659 Bernal, S., and Sabater, F. Changes in stream discharge and solute dynamics between
660 hillslope and valley-bottom intermittent streams. *Hydrol. Earth Syst. Sci.*, 16, 1595-
661 1605, 2012.

662 Bernal, S., von Schiller, D., Martí, E., Sabater, F. In-stream net uptake regulates
663 inorganic nitrogen export from catchment under base flow conditions. *J. Geophys.*
664 *Res.*, 117, G00N05, doi:10.1029/2012JG001985, 2012.

665 Bernhardt, E.S., Hall, R.O., and Likens, G.E. Whole-system estimates of nitrification
666 and nitrate uptake in streams of the Hubbard Brook experimental forest. *Ecosystems*,
667 5, 419-430, 2002.

668 Bernhardt, E.S., Likens, G.E., Buso, D.C., and Driscoll, C.T. In-stream uptake dampens
669 effects of major forest disturbance on watershed nitrogen export. *P. Natl. Acad. Sci.*
670 *USA*, 100, 10304-10308, 2003.

671 Bohlen, P.J., Groffman, P.M., Driscoll, C.T., Fahey, T.J., and Siccama, T.G. Plant-soil-
672 microbial interactions in a northern hardwood forest. *Ecology*, 82, 965-978, 2001.

673 Bormann, F.H. and Likens, G.E. Nutrient cycling. *Science*, 155, 424-429, 1967.

674 Brookshire, E.N.J., Valett, H.M., and Gerber, S.G. Maintenance of terrestrial nutrient
675 loss signatures during in-stream transport. *Ecology*, 90, 293-299, 2009.

676 Butturini, A., Bernal, S., Nin, E., Hellín, C., Rivero, L., Sabater, S., and Sabater, F.
677 Influences of stream groundwater hydrology on nitrate concentration in unsaturated
678 riparian area bounded by an intermittent Mediterranean stream. *Water Resour. Res.*,
679 39, 1110, doi:10.1029/2001WR001260, 2003.

680 Castro-Díez, P., Valle, G., González-Muñoz, N., Alonso, A. 2014. Can the life-history
681 strategy explain the success of the exotic trees *Ailanthus altissima* and *Robinia*
682 *pseudoacacia* in Iberian floodplain forests? *PLOS One* 9, doi:
683 10.1371/journal.pone.0100254.

684 Compton, J.E., Robbin Church, M., Larned S.T., and Hogsett, W.E. Nitrogen export
685 from forested watershed in the Oregon Coast Range: the role of N₂-fixing red alder.
686 *Ecosystems*, 6, 773-785, 2003.

687 Covino, T.P., and McGlynn, B.L. Stream gains and losses across a mountain-to-valley
688 transition: impacts on watershed hydrology and stream water chemistry. *Water*
689 *Resour. Res.*, 43, W10431, doi:10.1029/2006WR005544, 2007.

690 Covino, T.P., McGlynn, B.L., and Baker, M. Separating physical and biological nutrient
691 retention and quantifying uptake kinetics from ambient to saturation in successive
692 mountain stream reaches. *J. Geophys. Res.*, 115, G04010,
693 doi:10.1029/2009/JG001263, 2010.

694 Dent, C.L., and Grimm, N.B. Spatial heterogeneity of stream water nutrient
695 concentrations over successional time. *Ecology*, 80, 2283-2298, 1999.

696 Dent, C.L., Grimm, N.B. Martí, E., Edmonds, J.W., Henry, J.C., and Welter, J.R.
697 Variability in surface-subsurface hydrologic interactions and implications for
698 nutrient retention in an arid-land stream. *J. Geophys. Res.*, 112, G04004,
699 doi:10.1029/2007JG000467, 2007.

700 Ensign, S.H., and Doyle, M.W. Nutrient spiraling in streams and river networks. *J.*
701 *Geophys. Res.*, 111, G04009, doi:10.1029/2005JG00114, 2006.

702 Finlay, J. C., Hood, J. M., Limm, M. P., Power, M. E., Schade, J. D., and Welter, J. R..
703 Light-mediated thresholds in stream-water nutrient composition in a river network.
704 *Ecology*, 92, 140-150, 2011.

705 Gordon N.D., McMahon T.A., Finlayson B.L., Gippel, C.J., and Nathan, R.J. *Stream*
706 *hydrology: an introduction for ecologists*. Wiley, West Sussex, UK, 2004.

707 Groffman, P.M., Gold, A.J., and Simmons, R.C. Nitrate dynamics in riparian forests:
708 microbial studies. *J. Environ. Qual.*, 21, 666-671, 1992.

709 Harms, T.K., and Grimm, N.B. Hot spots and hot moments of carbon and nitrogen
710 dynamics in a semiarid riparian zone. *J. Geophys. Res.*, 113, G01020,
711 doi:10.1029/2007JG000588, 2008.

712 Hedin, L.O., von Fisher, J.C., Ostrom, N.E., Kennedy, B.P., Brown, M.G., and
713 Robertson, G.P. Thermodynamic constraints on nitrogen transformations and other
714 biogeochemical processes at soil-stream interfaces. *Ecology*, 79, 684-703, 1998.

715 Helfield, J.M., and Naiman, R.J. Salmon and alder as nitrogen sources to riparian
716 forests in a boreal Alaskan watershed. *Oecologia*, 133, 573-582, doi:
717 10.1007/s00442-002-1070-x, 2002.

718 Hill, A.R., Labadia, C.F., and Sanmugadas, K. Hyporheic zone hydrology and nitrogen
719 dynamics in relation to the streambed topography of a N-rich stream.
720 *Biogeochemistry*, 42, 285-310, 1998.

721 Hill, W.R., Mulholland, P.J., and Marzolf, E.R. Stream ecosystem response to forest
722 leaf emergence in spring. *Ecology*, 82, 2306-2319, 2001.

723 Houlton, B.Z., Driscoll, C.T., Fahey, T.J., Likens, G.E., Groffman, P.M., Bernhardt,
724 E.S., and Buso, D.C. Nitrogen dynamics in ice-storm-damaged forest ecosystems:
725 implications for nitrogen limitation theory. *Ecosystems*, 6, 431-443, 2003.

726 Institut Cartografic de Catalunya (ICC). Orthophotomap of Catalunya 1:25 000.
727 Generalitat de Catalunya. Departament de Política Territorial i Obres, 2010.

728 Jencso, K.G., McGlynn, B.L., Gooseff, M.N., Bencala, K.E., and Wondzell, S.M.
729 Hillslope hydrologic connectivity controls riparian groundwater turnover:
730 implications of catchment structure for riparian buffering and stream water sources.
731 *Water Resour. Res.*, 46, W10524, doi:10.1029/2009WR008818, 2010.

732 Johnson, C.E., Driscoll, C.T., Siccama, T.G., and Likens, G.E. Element fluxes and
733 landscape position in a northern hardwood forest watershed ecosystem. *Ecosystems*,
734 3, 159-184, 2000.

735 Jones, J.B. Jr., Fisher, S.G., and Grimm, N.B. Nitrification in the hyporheic zone of a
736 desert stream ecosystem. *J. North Am. Benthological Soc.*, 14, 249-258, 1995.

737 Keeney D.R., and Nelson D.W. Nitrogen-inorganic forms. *Methods of soil analysis*.
738 Part 2. In: *Agronomy Monograph 9*. ASA and SSSA. Madison, WI. pp. 643–698,
739 1982.

740 Lawrence, G.B., Lovett, G.M., and Baevsky, Y.H. Atmospheric deposition and
741 watershed nitrogen export along an elevational gradient in the Castkills Mountains,
742 New York. *Biogeochemistry*, 50, 21-43, 2000.

743 Lewis, D. B., Schade, J. D., Huth, A. K., and Grimm, N. B. The spatial structure of
744 variability in a semi-arid, fluvial ecosystem. *Ecosystems*, 9, 386-397, 2006.

745 Likens, G.E. and Buso, D.C. Variation in streamwater chemistry throughout the
746 Hubbard Brook Valley. *Biogeochemistry*, 78, 1-30, doi: 10.1007/s10533-005-2024-
747 2, 2006.

748 Lowrance, R., Altier, L. S., Newbold, J. D., Schnabel, R. R., Groffman, P. M., Denver,
749 J. M., Correl, D. L., Gilliam, J. W., Robinson, J. L., Brinsfield, R. B., Staver, K. W.,
750 Locas, W., and Todd, A. H. Water quality functions of riparian forest buffers in
751 Chesapeake Bay watersheds. *Environ. Manag.*, 21, 687-712, 1997.

752 Lupon, A., Martí, E., Sabater, F. and Bernal, S. Green light: gross primary production
753 influences seasonal stream N export by controlling fine-scale N dynamics. *Ecology*
754 (in review), 2015.

755 Martí, E., Fisher, S.G., Schade, J.D., and Grimm, N.B. Flood-frequency and stream-
756 riparian linkages in arid lands, in: *Streams and ground waters*. Jones, J.B. and
757 Mulholland, P.J. (Eds), Academic Press, London, UK, 2000.

758 Mayer, P.M., Reynolds, S.K., Marshall, Jr., McCutchen, D., and Canfield, T.J. Meta-
759 Analysis of nitrogen removal in riparian buffers. *J. Environ. Qual.* 36, 1172-1180,
760 doi:10.2134/jeq2006.0462, 2007.

761 McClain, M.E., Boyer, E.W., Dent, C.L., Gergel, S.E., Grimm, N.B., Groffman, P.M.,
762 Hart, S.C., Harvey, J.W., Johnston, C.A., Mayorga, E., McDowell, W.H., and Pinay,
763 G. Biogeochemical hot spots and hot moments at the interface of terrestrial and
764 aquatic ecosystems. *Ecosystems*, 6, 301–312, 2003.

765 Meyer, J. L., and Likens, G. E. Transport and transformation of phosphorus in a forest
766 stream ecosystem. *Ecology* 60, 1255-1269, 1979.

767 Mineau, M. M., Baxter, C. V., and Marcarelli, A. M. A non-native riparian tree
768 (*Elaeagnus angustifolia*) changes nutrient dynamics in streams. *Ecosystems*, 14, 353-
769 365, 2011.

770 Morrice, J.A., Valett, H.M., Dahm, C.N., and Campana, M.E.: Alluvial characteristics,
771 groundwater-surface water exchange and hydrological retention in headwaters
772 streams, *Hydrol. Process.*, 11, 253-267, 1997.

773 Murphy, J. and J.P. Riley. A modified single solution method for determination of
774 phosphate in natural waters. *Anal. Chim. Acta*, 27, 31-36, 1962.

775 Nadal-Sala, D, Sabaté, S., Sánchez-Costa, E., Boumghar, A., and Gracia, C.A.,
776 Different responses to water availability and evaporative demand of four co-
777 occurring riparian tree species in N Iberian Peninsula. Temporal and spatial sap flow
778 patterns. *Acta Hortic.* 991, 215-222, 2013.

779 Payn, R. A., Gooseff, M. N., McGlynn, B. L., Bencala, K. E., and Wondzell, S. M.
780 Channel water balance and exchange with subsurface flow along a mountain
781 headwater stream in Montana, United States. *Water Resour. Res.*, 45, W11427,
782 doi:10.1029/2008WR007644, 2009.

783 Peterson, B. J., Wollheim, W. M., Mulholland, P. J., Webster J. R., Meyer, J. L., Tank,
784 J. L., Martí, E., Bowden, W. B., Valett, H. M., Hershey, A. E., McDowell, W. H.,
785 Dodds, W. K., Hamilton, S. K., Gregory, S., and Morrall, D. D. Control of nitrogen
786 export from watersheds by headwater streams. *Science*, 292, 86–90, 2001.

787 Roberts, B.J., and Mulholland, P.J. In-stream biotic control on nutrient biogeochemistry
788 in a forested stream, West Fork of Walker Branch. *J. Geophys. Res.*, 112, G04002,
789 doi:10.1029/2007JG000422, 2007.

790 Ross, D.S., Shanley, J.B., Campbell, J.L., Lawrence, G.B., Bailey, S.W., Likens, G.E.,
791 Wemple, B.C., Fredriksen, G., and Jamison, A.E. Spatial patterns of soil nitrification
792 and nitrate export from forested headwaters in the northeastern United States. *J.*
793 *Geophys. Res.*, 117, G01009, doi: 10.1029/2011JG001740, 2012.

794 Sabater, S., Butturini, A., Clement, J.C., Burt, T., Dowrick, D., Hefting, M., Maître, V.,
795 Pinay, G., Postolache, C., Rzepecki, M., and Sabater, F. Nitrogen removal by
796 riparian buffers along a European climatic gradient: patterns and factors of variation.
797 *Ecosystems*, 6, 20-30, 2003.

798 Scanlon, T.M., Ingram, S.P., and Riscassi, A.L. Terrestrial and in-stream influences on
799 the spatial variability of nitrate in a forested headwater catchment. *J. Geophys. Res.*,
800 115, G02022, doi:10.1029/2009JG001091, 2010.

801 Starry, O. S., Valett, H. M., and Schreiber, M. E. Nitrification rates in a headwater
802 stream: influences of seasonal variation in C and N supply. *J. North Am.*
803 *Benthological Soc.*, 24, 753-768, 2005.

804 Stock, W.D., Wienand, K.T., and Baer, A.C. Impacts of invading N₂-fixing acacia
805 species on patterns of nutrient cycling in two Cape ecosystems: evidence from soil
806 incubation studies and ¹⁵N natural abundance values. *Oecologia*, 101, 375-382, 1995.

807 Strauss, E.A., and Lamberti, G.A. Regulation of nitrification in aquatic sediments by
808 organic carbon. *Limnol. Oceanogr.*, 45, 1854-1859, 2000.

809 Technicon. Technicon Instrument System, in : Technicon Method Guide, Technicon,
810 ed. Tarrytown, New York, 1976.

811 Uehlinger, U. Resistance and resilience of ecosystem metabolism in a flood-prone river
812 system. *Freshwater Biol.*, 45, 319-332, 2000.

813 Valett, H.M., Morrice, J.A., Dahm, C.N. and Campana, M.E. Parent lithology, surface-
814 groundwater exchange and nitrate retention in headwater streams. *Limnol.*
815 *Oceanogr.*, 41, 333-345, 1996.

816 Vidon, P., and Hill, A.R. Landscape controls in nitrate removal in stream riparian zones.
817 *Water Resour. Res.*, 40, W03201, doi:10.1029/2003WR002473, 2004.

818 Vidon, P.G.F., Craig, Al., Burns, D., Duval, T.P., Gurwick, N., Inamdar, S., Lowrance,
819 R., Okay, J., Scott, D., and Sebestyen, S. Hot spots and hot moments in riparian
820 zones: potential for improved water quality management. *J. Am. Water Resour.*
821 *Assoc.*, 46, 278-298, 2010.

822 von Schiller, D., Bernal, S., and Martí, E. A comparison of two empirical approaches to
823 estimate in-stream net nutrient uptake. *Biogeosciences*, 8, 875-882, 2011.

824 von Schiller, D., Bernal, S., Sabater, S., and Martí, E. A round-trip ticket: the
825 importance of release processes for in-stream nutrient spiraling. *Freshwater Science*,
826 DOI: 10.1086/679015, 2015.

827 Wollheim, W. M., Vörösmarty, C. J., Peterson, B. J., Seitzinger, S. P., and Hopkinson,
828 C. S. Relationship between river size and nutrient removal. *Geophys. Res. Lett.*, 33,
829 L06410, doi:10.1029/2006GL025845, 2006.

830 Zar, J. H. *Biostatistical analysis*. Prentice-Hall/Pearson, Ed. 5th Edition. Upper Saddle
831 River, N.J., 2010.

832 **Tables**

833 **Table 1.** Median and interquartile range [25th, 75th percentiles] of stream and riparian
 834 groundwater solute concentrations for the dormant and vegetative period. The number
 835 of cases is shown in parenthesis for each group. For each variable, the asterisk indicates
 836 statistically significant differences between the two water bodies (Wilcoxon paired rank
 837 sum test, $p < 0.01$).

		Stream	Riparian groundwater
Dormant	Cl ⁻ (mg L ⁻¹)	7.6 [6.5, 8] (60)	7.7 [7.2, 8.8] (57)*
	N-NO ₃ ⁻ (μg N L ⁻¹)	192 [159, 262] (60)	194 [109, 298] (56)
	N-NH ₄ ⁺ (μg N L ⁻¹)	8.9 [6.5, 10.3] (60)	19 [13.8, 34.2] (56)*
	SRP (μg P L ⁻¹)	7.6 [4.5, 11.7] (60)	8 [6, 20] (51)
	DO (mg L ⁻¹)	12.9 [11.5, 16] (60)	3.5 [1.5, 4.6] (54)*
Vegetative	Cl ⁻ (mg L ⁻¹)	8.8 [7.9, 13.5] (100)	10.1 [8.6, 15] (98)*
	N-NO ₃ ⁻ (μg N L ⁻¹)	223 [155, 282] (102)	168 [77, 264] (98)*
	N-NH ₄ ⁺ (μg N L ⁻¹)	10 [8.7, 12.8] (103)	27 [18.2, 37.1] (101)*
	SRP (μg P L ⁻¹)	16.5 [11.7, 21.3] (103)	14.1 [9.3, 23.3] (97)
	DO (mg L ⁻¹)	9.9 [9.1, 11.1] (84)	1.7 [0.8, 2.5] (98)*

839

840 **Table 2.** Spearman ρ coefficient between stream water and riparian groundwater solute
 841 concentrations for each period and for the whole data set collected at the Font del Regàs
 842 during the study period. The relative root mean square error (RRMSE) indicates
 843 divergences from the 1:1 line. The number of cases is shown in parenthesis for each
 844 variable. ns, no significant.

	Dormant			Vegetative			All data		
	ρ	RRMSE (%)	n	ρ	RRMSE (%)	n	ρ	RRMSE (%)	n
Cl ⁻	0.78*	2.1	53	0.8*	2.9	98	0.84*	2.8	151
N-NO ₃ ⁻	0.48*	8.1	57	0.34*	8.3	101	0.37*	6	158
N-NH ₄ ⁺	ns	11.7	57	ns	9.1	101	ns	7.3	158
SRP	ns	17.9	57	0.43*	5.5	101	0.41*	7.3	158

845 *p<0.001

846

847

848 **Table 3.** Median and interquartile range [25th, 75th percentile] of in-stream net nutrient
 849 uptake flux (F_{sw}) and the potential of F_{sw} to modify solute input fluxes ($|F_{sw} \cdot x / F_{in}|$) for
 850 the two spatial scales considered (stream segment and whole reach) during the study
 851 period. n = 150 and 10 for segments and whole-reach data sets, respectively.

		By segment	By whole reach
F_{sw} ($\mu\text{g m}^{-1} \text{s}^{-1}$)	Cl^-	6 [-37, 80]	12 [2, 33]
	N- NO_3^-	-0.43 [-4.4, 1.3]	-0.97 [-3.4, 1.6]
	N- NH_4^+	0.17 [-0.06, 0.63]	0.2 [-0.02, 1.1]
	SRP	0 [-0.6, 0.21]	-0.06 [-0.21, 0.01]
$ F_{sw} \cdot x / F_{in} $ (%)	Cl^-	3 [1, 10]	4 [2, 9]
	N- NO_3^-	6 [2, 14]	24 [8, 67]
	N- NH_4^+	18 [9.5, 35]	48 [25, 71]
	SRP	20.5 [3.4, 41]	15.5 [6, 66]

852

853

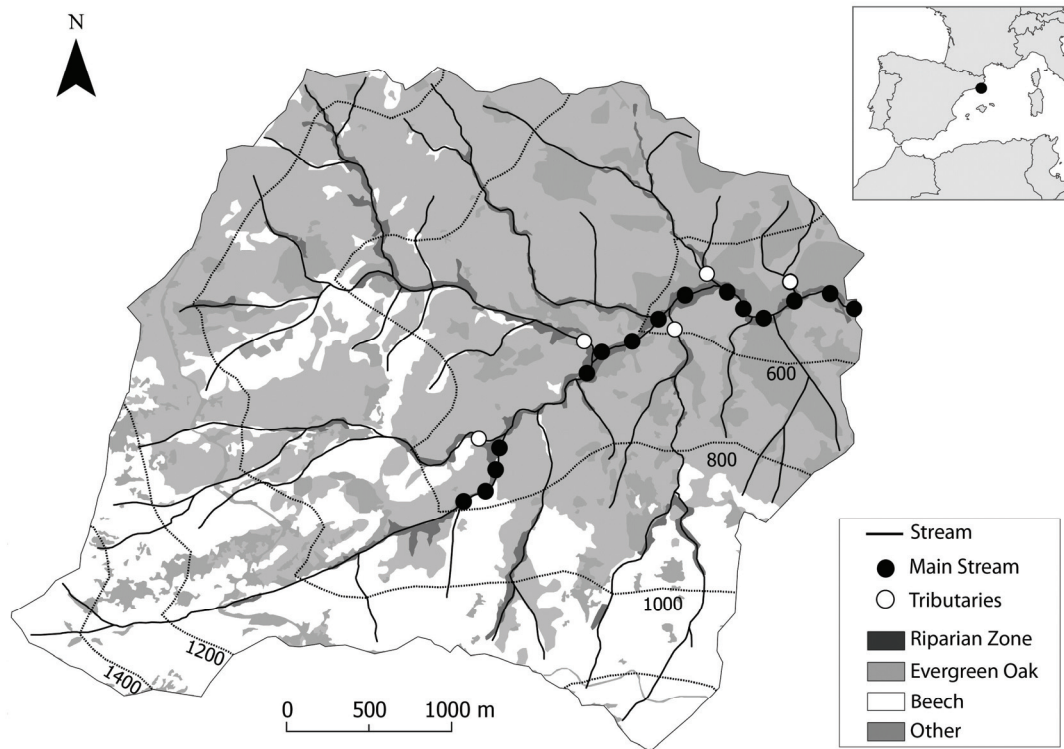
854 **Table 4.** Median and interquartile range [25th, 75th percentile] of the relative
855 contribution of inputs from upstream (F_{top}/F_{in}), net riparian groundwater
856 ($(F_{gw} > 0)/F_{in}$), tributaries (F_{ef}/F_{in}), and in-stream release ($|(F_{sw} < 0)/F_{in}|$) to stream
857 solute fluxes at the whole-reach scale. Note that relative contributions from different
858 sources do not up to 100% because they are medians rather than means. For each solute,
859 different letters indicate statistically significant differences between solute sources
860 (Mann Whitney test with post-hoc Tukey test, $p < 0.01$). $n = 10$ for the 4 solutes.

<i>Relative contribution (%)</i>	Cl^-	$N-NO_3^-$	$N-NH_4^+$	SRP
Upstream	15 [12, 17] ^B	22 [20, 35] ^A	8 [6, 13] ^{BC}	11 [6, 17] ^B
Riparian Groundwater	28 [14, 38] ^B	17 [5, 47] ^A	63 [43, 75] ^A	21 [7, 38] ^{AB}
Tributaries	59 [46, 69] ^A	22 [19, 24] ^A	21 [17, 30] ^B	34 [26, 50] ^A
861 In-stream Release	0 [0, 0.3] ^C	22 [0, 50] ^A	0 [0, 6] ^C	19 [0, 55] ^B

862

863

864 **Figures**



865

866

867 **Figure 1.** Map of the Font del Regàs catchment within the Montseny Natural Park (NE,

868 Spain). The vegetation cover and the main stream sampling stations along the 3.7-km

869 reach are indicated. There were 5 and 10 sampling stations along the 2nd and 3rd order

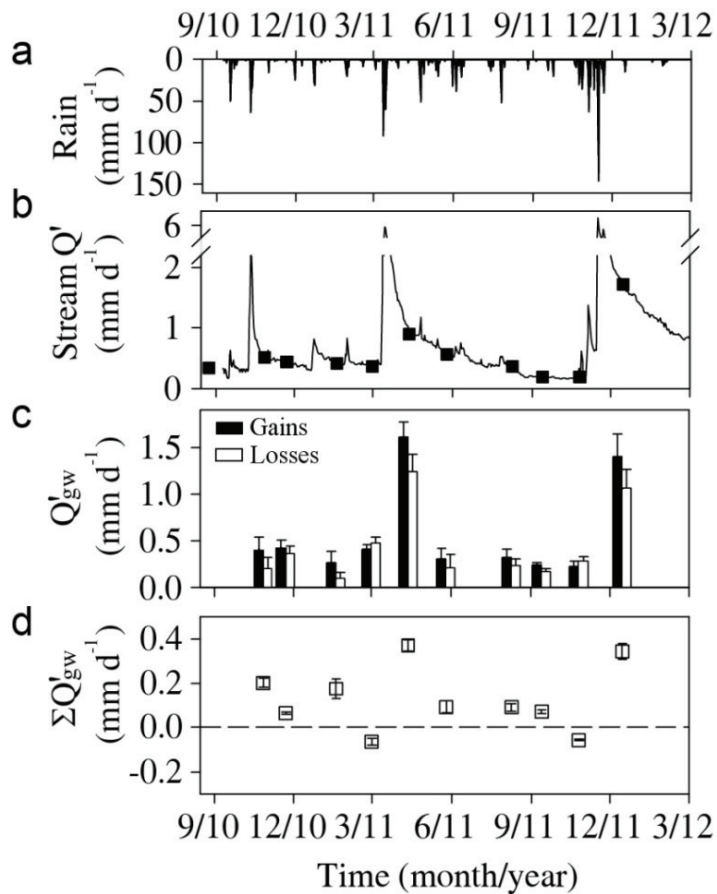
870 sections, respectively. Four permanent tributaries discharged to the main stream from

871 the upstream- to the downstream-most site (white circles). Additional water samples

872 were collected from a small tributary draining through the inhabited area at the lowest

873 part of the reach. The remaining tributaries were dry during the study period.

874

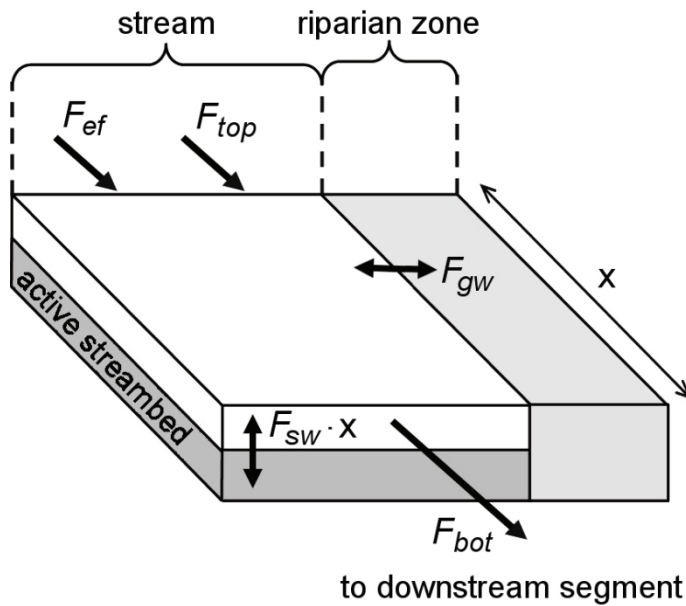


875

876 **Figure 2.** Temporal pattern of area-specific (a) rainfall, (b) stream discharge, (c) whole-
 877 reach gross hydrological gains and losses, and (d) cumulative net groundwater inputs at
 878 the downstream-most site. Black squares in (b) are dates of field campaigns. Error bars
 879 in (c) and (d) show the uncertainty associated with the empirical estimation of Q from
 880 tracer slug additions. Error bars in (b) are smaller than the symbol size.

881

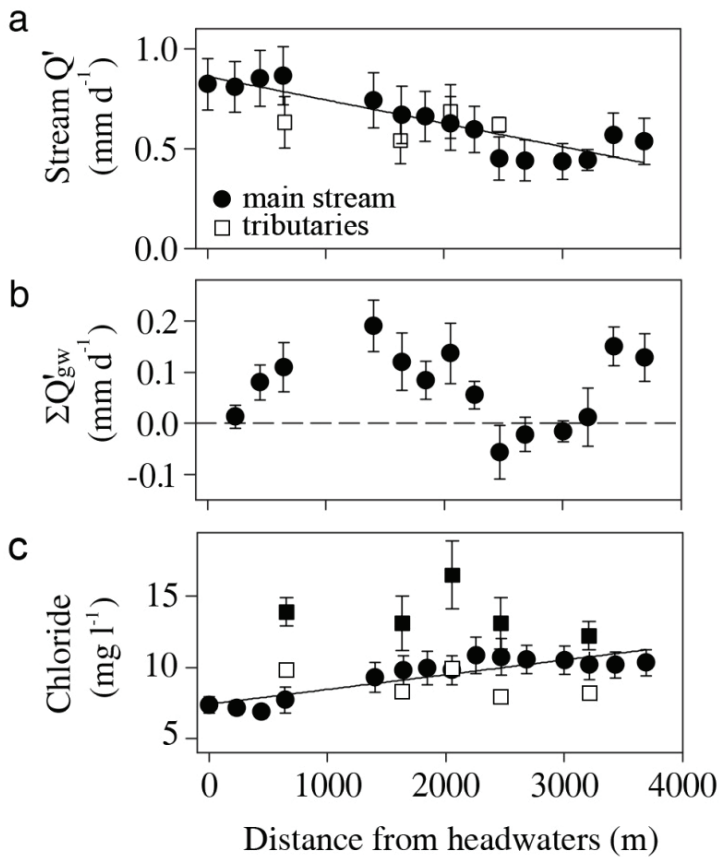
882



883

884 **Figure 3.** Conceptual representation of nutrient fluxes considered to estimate in-stream
885 net nutrient uptake for each stream segment ($F_{sw} \cdot x$, Equation 2). For each segment of
886 length x , the considered nutrient input fluxes were upstream (F_{top}) and tributaries (F_{ef}).
887 Nutrient fluxes exiting the stream segment (F_{bot}) were F_{top} for the contiguous
888 downstream segment. Riparian groundwater nutrient fluxes could either enter ($F_{gw} > 0$)
889 or exit ($F_{gw} < 0$) the stream. Nutrient fluxes for each component were estimated by
890 multiplying its water flux (Q) by its nutrient concentration (C). In-stream net nutrient
891 uptake ($F_{sw} \cdot x$) is the result of gross nutrient uptake and release by the active streambed.
892 $F_{sw} \cdot x$ can be positive (gross uptake $>$ release), negative (gross uptake $<$ release), or nil
893 (gross uptake \sim release). See text for details.

894

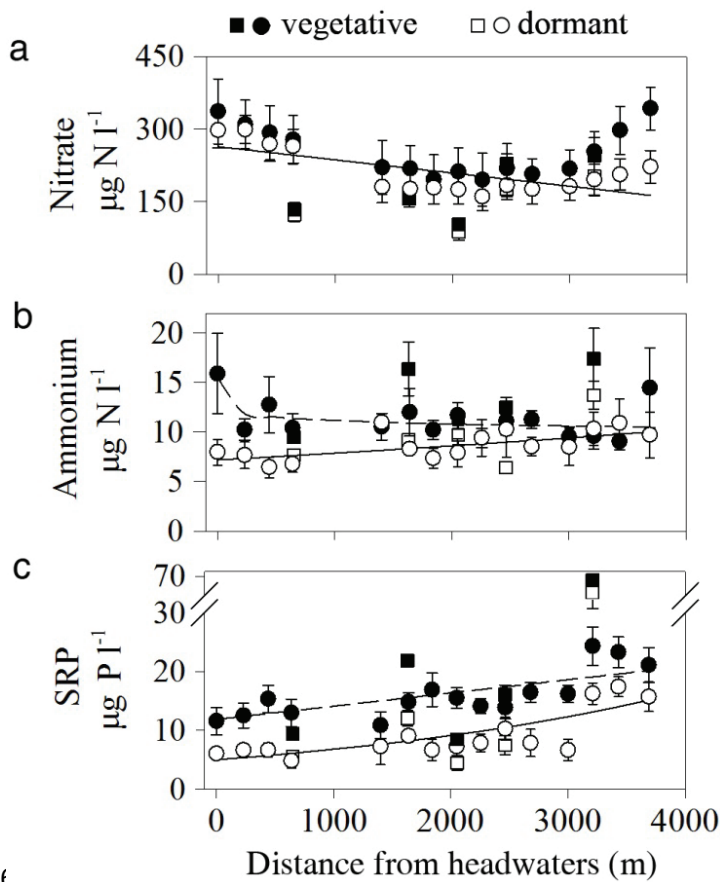


896

897 **Figure 4.** Longitudinal pattern of (a) area-specific stream discharge, (b) cumulative
 898 area-specific net groundwater inputs along the reach, and (c) stream chloride
 899 concentration. Symbols are average and standard error (whiskers) for the study period.
 900 Squares are values for tributaries. Stream chloride concentration in tributaries is shown
 901 separately for the dormant (white) and vegetative (black) period. Tributaries showed no
 902 differences in discharge between the two periods. Model regressions are indicated with
 903 a solid line only when significant (tributaries not included in the model).

904

905

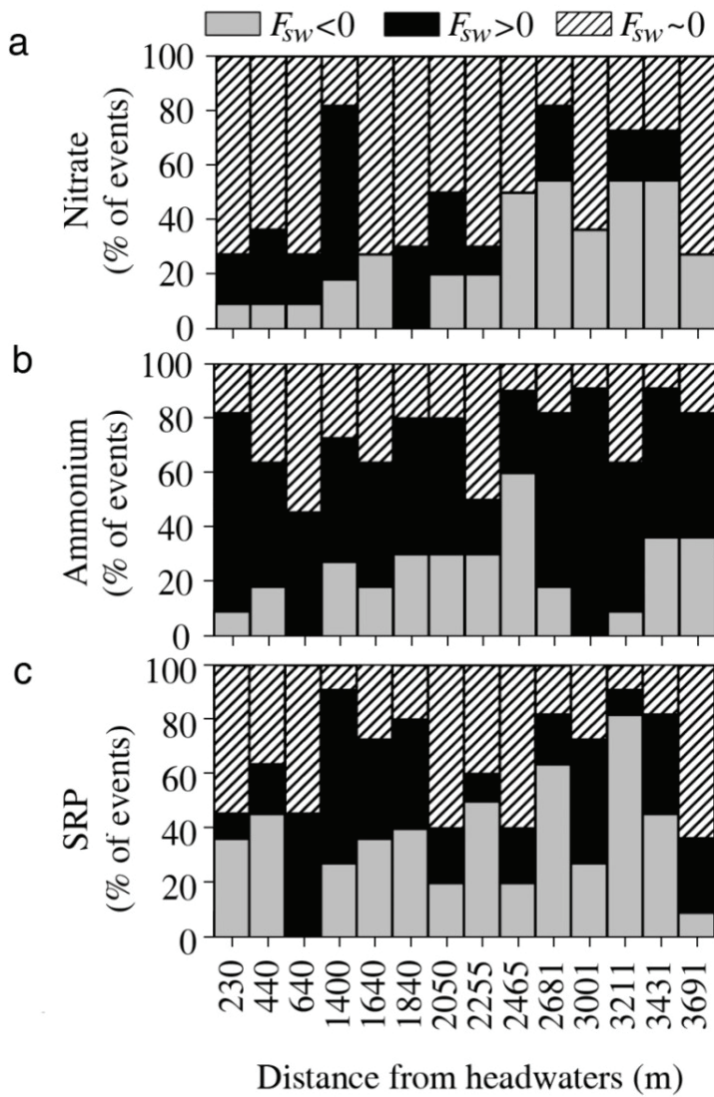


906

907

908 **Figure 5.** Longitudinal pattern of stream nutrient concentrations for (a) nitrate, (b)
909 ammonium, and (c) solute reactive phosphorus at Font del Regàs. Symbols are average
910 and standard error (whiskers) for the main stream (circles) and tributaries (squares).
911 Lines indicate significant longitudinal trends for the dormant (solid) and vegetative
912 (dashed) period (tributaries not included in the model).

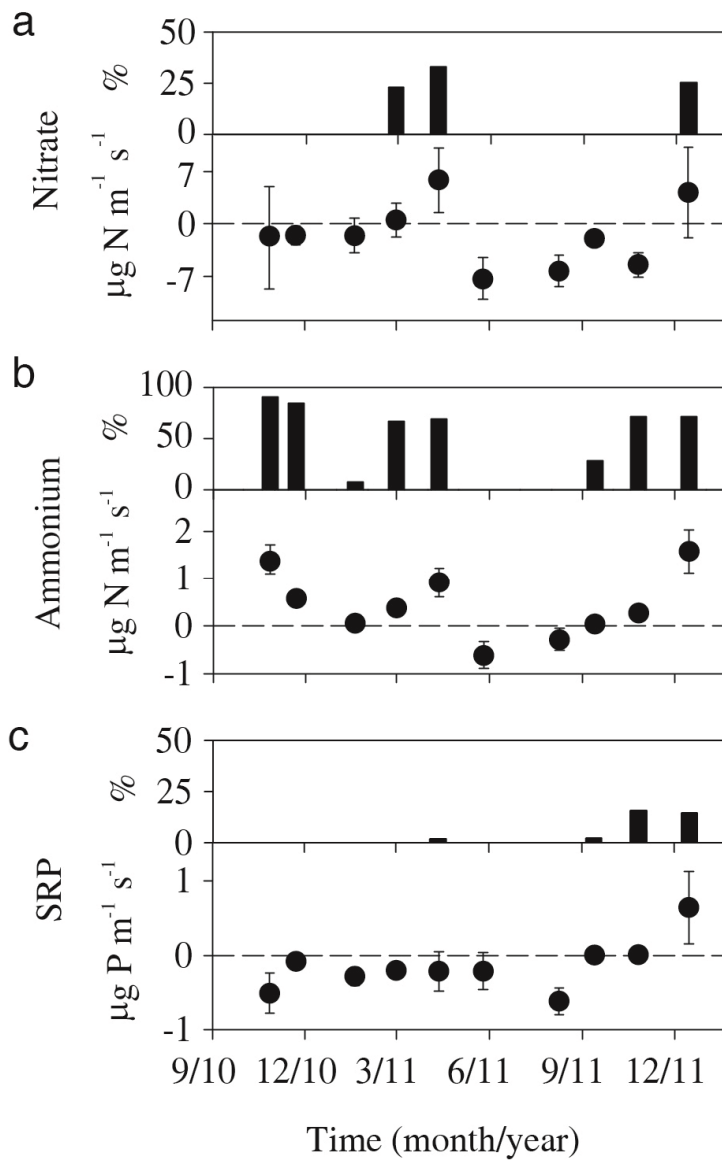
913



915

916 **Figure 6.** Frequency of dates for which $F_{sw} < 0$ (gross uptake < release), $F_{sw} > 0$ (gross
 917 uptake > release), and $F_{sw} \sim 0$ (gross uptake ~ release) for (a) nitrate, (b) ammonium,
 918 and (c) soluble reactive phosphorus for the 14 contiguous segments along the study
 919 reach from August 2010 to December 2011 (n = 11). The frequency is expressed as
 920 number of events in relative terms.

921



923

924 **Figure 7.** Temporal pattern of in-stream net nutrient uptake (F_{sw} , in $\mu\text{g m}^{-1} \text{s}^{-1}$) for (a)

925 nitrate, (b) ammonium, and (c) soluble reactive phosphorus at the whole-reach scale.

926 Whiskers are the uncertainty associated with the estimation of stream discharge from

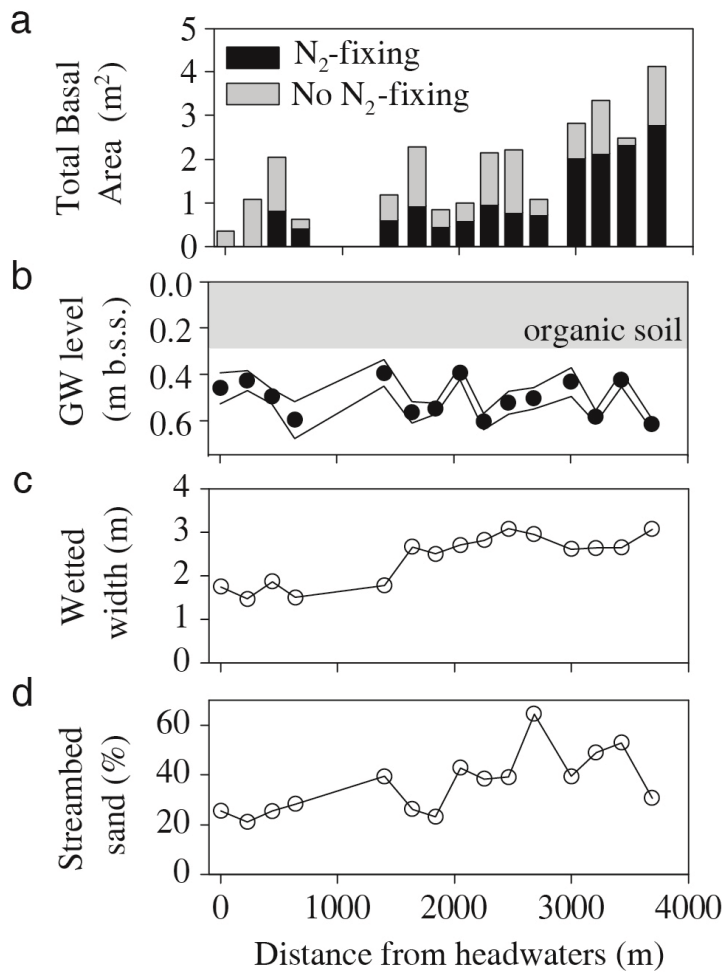
927 slug tracer additions. $F_{sw} > 0$ indicates that gross uptake prevailed over release, while928 $F_{sw} < 0$ indicates the opposite. For those cases for which $F_{sw} > 0$, the contribution of in-929 stream net nutrient uptake to reduce stream nutrient fluxes ($F_{sw} \cdot x/F_{in}$, in %) is shown

930 (black bars).

931

932

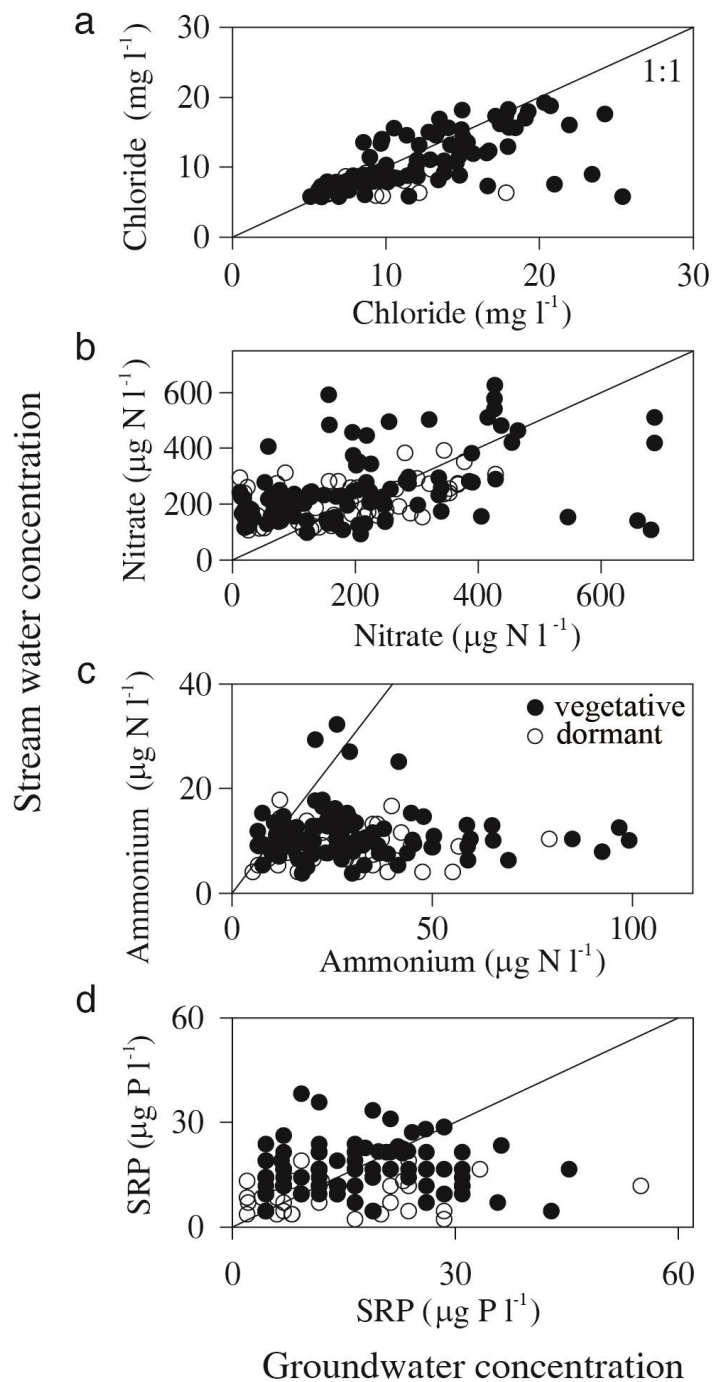
933 **Supplementary Figures**



934

935 **Figure S1.** (a) Total basal area of riparian trees, (b) mean riparian groundwater level (in
936 m below the soil surface), (c) stream wetted width, and (d) percentage of sands in
937 streambed for each sampling site along the study reach. Different colors in (a) indicate
938 the basal area of N₂- and no N₂-fixing trees. The solid lines in (b) are the 95% lower and
939 upper values of the riparian groundwater level.

940



941

942 **Figure S2.** Relationship between riparian groundwater and stream water concentrations
 943 for (a) chloride, (b) nitrate, (c) ammonium, and (d) soluble reactive phosphorus at each
 944 sampling site and for each sampling date at Font del Regàs. The 1:1 line is indicated in
 945 black.